Molecular Crystals and Liquid Crystals Incorporating Nonlinear Optics

Publication details, including instructions for authors and subscription information:
http://www.tandfonline.com/loi/gmcl17

Determination of Third-Order Nonlinear Optical Susceptibilities for Organic Materials by Third-Harmonic Generation

K. Kubodera [a] & H. Kobayashi [a]

[a] NTT Opto-electronics Laboratories, Atsugi-shi, Kanagawa, 243-01, Japan

Version of record first published: 04 Oct 2006.

To cite this article: K. Kubodera & H. Kobayashi (1990): Determination of Third-Order Nonlinear Optical Susceptibilities for Organic Materials by Third-Harmonic Generation, Molecular Crystals and Liquid Crystals Incorporating Nonlinear Optics, 182:1, 103-113

To link to this article: http://dx.doi.org/10.1080/00268949008047792

Mol. Cryst. Liq. Cryst., 1990, Vol. 182A, pp. 103–113
Reprints available directly from the publisher
Photocopying permitted by license only

Printed in the United States of America

Determination of Third-Order Nonlinear Optical Susceptibilities for Organic Materials by Third-Harmonic Generation

K. KUBODERA and H. KOBAYASHI

NTT Opto-electronics Laboratories, Atsugi-shi, Kanagawa 243-01, Japan

(*Received May 6, 1989; accepted for publication June 5, 1989*)

Third-order optical nonlinearities have been evaluated for organic materials in powder, solution, and film forms, by third-harmonic generation (THG) measurement. Considerations of the effects of THG interference between film sample and substrate, and of the effect of THG in air, are made for an accurate $\chi^{(3)}$ evaluation. Several types of monomeric and polymeric materials are examined by this method.

Keywords: THG Measurement, $\chi^{(3)}$, π-conjugated polymers, polydiacetylene.

1. INTRODUCTION

Recently, much interest has been concentrated on organic materials as third-order non linear optical materials because some organic materials with conjugated π-electrons show remarkably large nonlinearities.[1,2] Among several types of third-order nonlinear optical materials which show intensity-dependent refractive indices, organic materials have the advantages of very fast response times and low absorption losses compared to semiconductor materials. These characteristics make organic materials desirable for use in ultrafast non linear optical devices, such as optically gated optical switches and optical bistable devices, which will be key components in future optical systems.[3,4]

For the evaluation of third-order nonlinearities for organic materials, several methods have been developed, such as degenerate four-wave mixing,[5,6] third-harmonic generation (THG),[7,8] nonlinear etalon measurement,[9] waveguide mode observation,[10,11] and etalon spectrum analysis with an applied DC voltage.[12] THG measurement is the easiest method of these, and the efficiency of the coherent process is easily evaluated without the intrusion of thermal or other absorptive nonlinear-optical processes.

This paper describes the evaluation of third-order nonlinear optical susceptibilities for organic materials by THG measurement. The evaluation technique is applied to various monomeric and polymeric samples in powder, solution, and film states. Measurement accuracy is best for film samples. To improve further the accuracy of the film measurement, considerations were made on the interference effects of third-harmonic waves between the sample and the substrate, or the sample and air.

2. THG MEASUREMENT SYSTEM

THG measurements were performed at pump wavelength around 1.9 μm using lithium niobate ($LiNbO_3$) difference-frequency generation between a Q-switched Nd:YAG laser and a tunable dye laser.[13] Since organic materials in this experiment have absorption edges in the 0.5–0.7 μm wavelength region, this pump wavelength corresponds to the nonresonant or near-resonant region of three-photon resonance. Pump pulse duration was 5.5 ns, repetition rate was 10 Hz, and peak pump power density was 80–200 MW/cm^2.

For powder materials, samples were prepared by placing powders to about 1 mm thickness on a microscope slide; these were held by adhesive tape. A particle size fraction in the range 88–105 μm was prepared using standard sieves. Pump light was allowed to impinge onto the powders through the glass slide. THG radiation backscattered from the powders was collected by a condenser lens. The intensity of THG radiation passing through an IR absorptive filter was measured by a photomultiplier and an oscilloscope.

For film materials, samples were mounted on a goniometer and rotated about an axis perpendicular to the laser beam. THG light passing through the sample was measured by an IR absorptive filter, a photomultiplier, and a boxcar averager. THG intensity patterns as a function of incident angle were analyzed to determine $\chi^{(3)}$ values and coherence lengths of the materials. Pump light polarization direction was adjusted to be parallel to the rotation axis.

Sample solutions were poured into a 1 mm thick glass cell. The setup for the THG measurement was the same as for film samples.

3. POWDER AND SOLUTION SAMPLE MEASUREMENT

Figure 1 shows THG intensities for some organic powder materials as a function of pump wavelength. As for powder materials, 4-dimethylamino-4′-nitrostilbene (DANS),[14] 4-diethylamino-4′-nitrostilbene (DEANS),[15] and para-nitroaniline (pNA)[16] were examined. A powder sample of PTS-polydiacetylene [bis-(*p*-toluene sulfonate) of 2,4-hexadiyne-1,6-diol], whose $\chi^{(3)}$ value has been reported,[17] was also prepared for comparison. Measured THG intensities were normalized by that for pNA at a wavelength $\lambda_p \approx 1.90$ μm. THG intensity for PTS decreases with decreasing pump wavelength due to reabsorption of the third harmonic wave, corresponding to the absorption edge wavelength of $\lambda_g \approx 0.65$ μm. On the other hand,

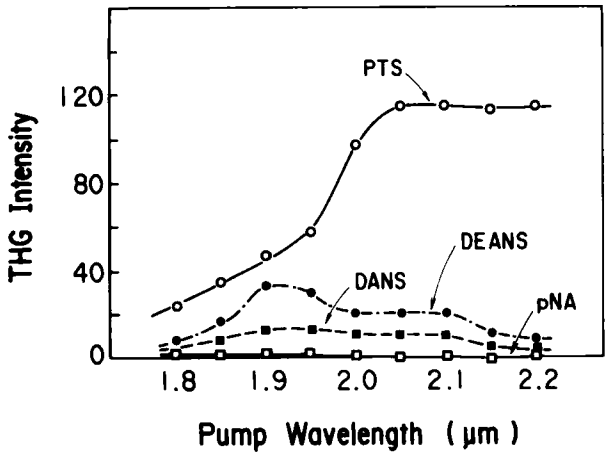

FIGURE 1 THG intensity spectra for powder samples of SHG inactive materials.

monomeric materials having a much better transparency in the range 0.6–0.65 μm, show almost constant THG intensities in this pump wavelength region.

THG intensity of powder samples can be expressed as

$$I_{3w} \propto \hat{l}_c^2 \{\hat{\chi}^{(3)}\}^2, \tag{1}$$

where $\hat{l}_c$ is the THG coherence length and $\hat{\chi}^{(3)}$ is the third order susceptibility, both averaged over the crystal orientations of powder samples. It follows that it is not possible to determine $\hat{\chi}^{(3)}$ values from measured THG intensities without knowing the averaged $\hat{l}_c$ values for each sample. Relative $\hat{\chi}^{(3)}$ values, simply calculated from Equation (1) by neglecting the difference in $\hat{l}_c$ values, are summarized in Table I, for qualitative information.

Figure 2 shows measured THG intensities for powder samples of 2-methyl-4-nitroaniline (MNA)[18] and trans-4′-dimethylamino-*N*-methyl-4-stilbazolium methylsulfate (DMSM).[19] These two samples have activities of second harmonic generation (SHG) in contrast to the materials in Figure 1. SHG intensities normalized by that of urea at pump wavelength of 1.90 μm are also shown in Figure 2. It is characteristic that THG intensities for these samples are much larger than those for SHG-inactive materials (Figure 1). However, it is reasonable to assume that measured THG intensities are principally caused by the cascading $\chi^{(2)}$ process ($\omega + \omega \rightarrow 2\omega$, $2\omega + \omega \rightarrow 3\omega$) because SHG and THG spectra in Figure 2 have very similar patterns to each other. To confirm this opinion, THG measurement was also performed for the solution state of these SHG-active materials.

Table I summarizes the results of $\chi^{(3)}$ evaluation for the above powder and solution measurements. For solution measurements, 5% (*m*/*m*) solutions in dimethylformamide (DMF) solvent were prepared. The method of $\chi^{(3)}$ determination is described in section 4.1. It is found that SHG-active materials should be rightly evaluated not by powder THG but by solution THG. It is also clear from Table I that monophenyl systems such as pNA and MNA show much lower $\chi^{(3)}$ values than diphenyl systems such as DMSM, DANS, and DEANS.

TABLE I

Results of $\chi^{(3)}$ evaluation for powder and solution samples. Pump wavelength λ_p = 1.90 μm.

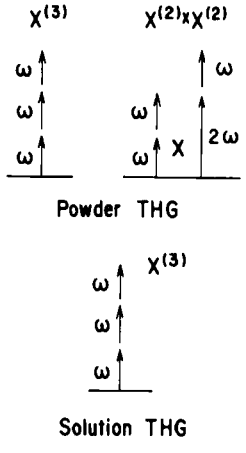

λ_p= 1.9 μm

	Powder THG $\hat{\chi}^{(3)}$(Relative)	Solution THG+ $\chi^{(3)}$(esu)
pNA	1	2.6×10^{-14}
MNA	(15.2)	2.9×10^{-14}
DMSM	(21.9)	11.8×10^{-14}
DANS	3.5	–
DEANS	5.7	–
PTS	10.7*	–

+ 5 wt % / DMF

* at λ_p=2.05 μm

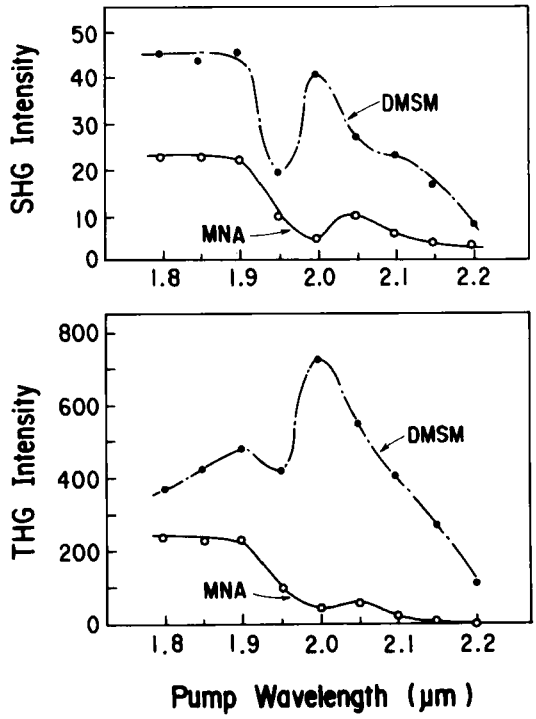

FIGURE 2 THG intensity spectra for powder samples of SHG active materials.

4. FILM SAMPLE MEASUREMENT

4.1 Determination of $\chi^{(3)}$ values

Figure 3 shows typical examples of THG intensity patterns from film samples as a function of incident angle. When film thickness l is much larger than THG coherence length (l_c of a few micrometers), a Maker fringe pattern is observed [Figure 3(a)], corresponding to consecutive optical pathlength variation. On the other hand, when l is much less than l_c, a monotonously decreasing pattern is observed [Figure 3(b)]. Figure 3(c) is the THG intensity pattern from a 1 mm thick silica (SiO_2) glass which is used as the standard sample.

The $\chi^{(3)}$ value of the film sample was determined according to the following simple equations, comparing THG intensity with the standard sample:

$$\chi^{(3)} = \chi_s^{(3)} (I_{3\omega}^{1/2}/l_c)/(I_{3\omega,s}^{1/2}/l_{c,s}) \qquad \text{for } l \gg l_c, \tag{2}$$

$$\chi^{(3)} = (2/\pi)\, \chi_s^{(3)} (I_{3\omega}^{1/2}/l)/(I_{3\omega,s}^{1/2}/l_{c,s}) \qquad \text{for } l \ll l_c \tag{3}$$

where $I_{3\omega}$ and $I_{3\omega,s}$ are THG peak intensities from film sample and standard sample, respectively (extrapolated maximum value in the case of a Maker fringe), l and l_c

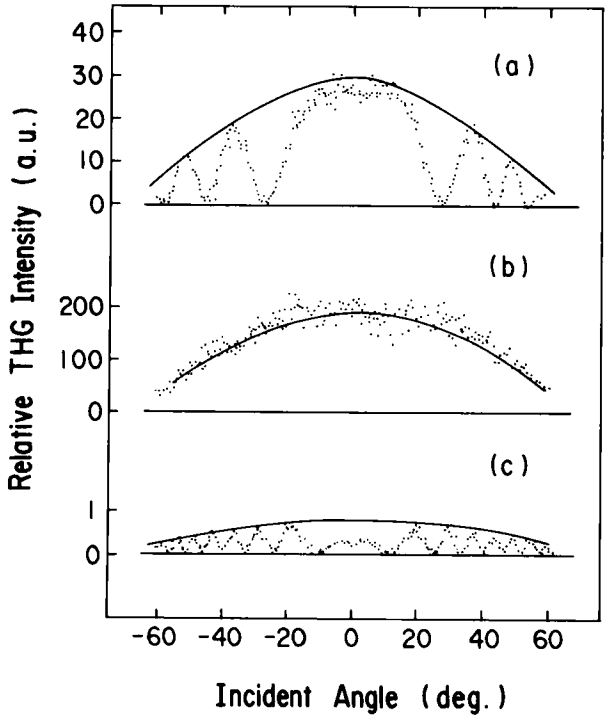

FIGURE 3 Typical THG intensity patterns as a function of incident angle. (a) a thick film sample: l = 290 μm, $\chi^{(3)} = 3.7 \times 10^{-13}$ esu, (b) a thin film sample: l = 0.69 μm, $\chi^{(3)} = 7.8 \times 10^{-12}$ esu, (c) standard SiO_2 glass sample: l = 1 mm.

are film thickness and coherence length of the sample, respectively, and $l_{c,s} = 18.1$ μm and $\chi_s^{(3)} = 2.8 \times 10^{-14}$ esu are l_c value and $\chi^{(3)}$ value for the standard sample of 1 mm thick silica glass at $\lambda_p = 1.90$ μm, respectively.[20] The refractive index difference between the film sample and silica glass was neglected in this calculation. All measurements were made in air at room temperature.

4.2 Consideration of Interference Effect between Film and Substrate

Especially for very thin film samples on glass substrates, where glass THG is comparable to film THG as shown in Figure 4, the interference effect was theoretically analyzed as follows.

Third harmonic electric fields from the film and the substrate, illustrated in Figure 5(a), are expressed as

$$E_{3\omega,f} = -(i\,\omega/n_f\,c)\,\chi^{(3)}\,E_\omega^3\,l \qquad (l \ll l_c), \tag{4}$$

$$E_{3\omega,\mathrm{sub}} = -(\omega/\pi\,n_{\mathrm{sub}}\,c)\,\chi_{\mathrm{sub}}^{(3)}\,E_\omega^3\,l_{c,\mathrm{sub}}\,[\exp(i\,\pi\,l_{\mathrm{sub}}/l_{c,\mathrm{sub}}) - 1], \tag{5}$$

where E_ω is the electric field of the pump light; n_f, $\chi^{(3)}$, and l are the refractive index, third order susceptibility, and sample thickness of the film, respectively; n_{sub}, $\chi_{\mathrm{sub}}^{(3)}$, and l_{sub} are those of the substrate, respectively; and $l_{c,\mathrm{sub}}$ is the coherence length of the substrate. Sample thickness l was assumed to be much less than the

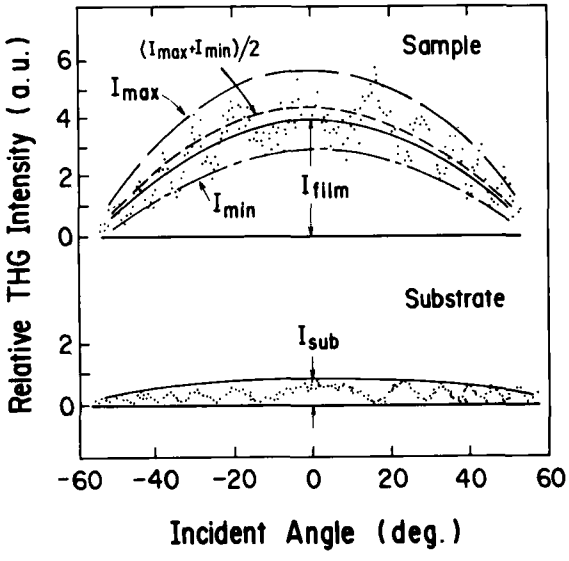

FIGURE 4 THG intensity pattern for a very thin film sample: $l = 0.08$ μm, $\chi^{(3)} = 1.4 \times 10^{-11}$ esu, $\lambda_p = 1.90$ μm.

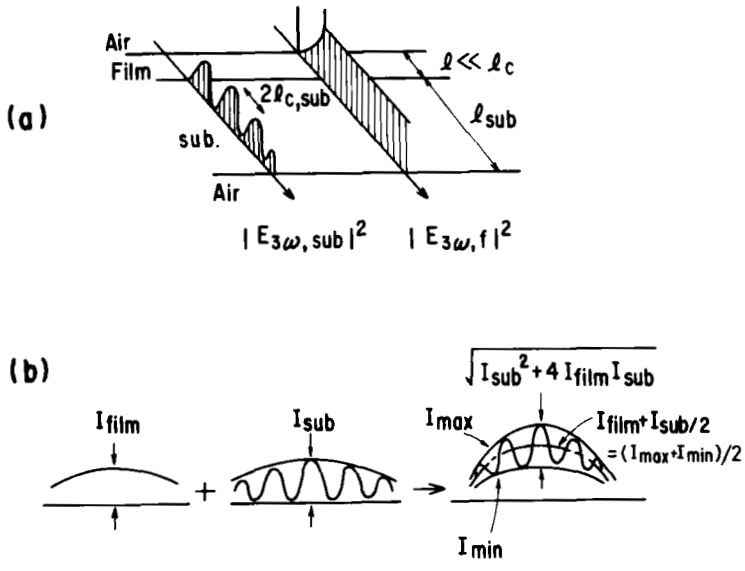

FIGURE 5 Analysis of THG interference between film and substrate.

film coherence length ($l << l_c$) in this calculation. Total THG intensity $I_{3\omega}$ is given by

$$I_{3\omega} \propto |E_{3\omega,f} + E_{3\omega,sub}|^2 \tag{6}$$

$$\propto I_{film} + I_{sub} \sin^2(\pi\, l_{sub}/2\, l_{c,sub}) + (I_{film}\, I_{sub})^{1/2} \sin(\pi\, l_{sub}/l_{c,sub}) \tag{7}$$

$$= (I_{film} + I_{sub}/2) + [(I_{sub}^2 + 4 I_{film}\, I_{sub})^{1/2}/2] \sin[(\pi\, l_{sub}/l_{c,sub}) - \psi], \tag{8}$$

where $I_{film} = \{\chi^{(3)}\}^2\, l^2$ is the THG intensity from the film, $I_{sub} = (4/\pi^2)\{\chi^{(3)}_{sub}\}^2\, l^2_{c,sub}$ is the envelope of the THG intensity pattern from the glass substrate, and ψ is the phase difference of the fringe pattern. The refractive index difference between the film and substrate was also neglected in this calculation. The last term in Equation (7) represents the interference effect between the film and substrate. The result, expressed by Equation (8), is illustrated in Figure 5(b).

From Equation (8) and Figure 5(b), it is easily seen that calibration can be done from the following very simple equation:

$$I_{film} = (I_{max} + I_{min})/2 - I_{sub}/2, \tag{9}$$

where I_{max} and I_{min} are envelopes of the superimposed THG intensity pattern.

The ultimate accuracy of this measurement is considered to be $\chi^{(3)}_{limit}\, l = 3 \times 10^{-13}$ esu μm, derived from the relation $I_{film} \approx I_{sub}$.

4.3 Consideration of air effect

It has been pointed out that the THG from air influences the measurement of small $\chi^{(3)}$ materials, such as silica glass,[7,21] which was used as the standard sample in our measurement. Although the $\chi^{(3)}$ value of air is small, THG from air is not negligible because of its very long coherence length. This air THG effect was examined experimentally in our measurement system. Figure 6 shows the measured THG peak intensities of Maker fringe patterns for a 1 mm thick silica glass as a function of the surrounding air pressure. In this measurement, a wedge-shaped glass sample was set at the center of a small vacuum chamber of 75 mm long, and the pump beam was allowed to impinge on the sample through a glass window. Maker fringe patterns were obtained in this case by moving the vacuum chamber with a goniometer perpendicularly to the pump beam. Condenser lenses having different focal lengths were used to focus the pump beam of about 2 mm diameter to a spot of 230 μm in diameter (in the case of f = 50 mm).

As shown in Figure 6, THG peak intensities decrease with increasing air pressure due to the phase difference of the third-harmonic lights from the sample and air. However, it is found that a shorter focal length produces a smaller air THG effect. This is presumably due to the relatively shorter THG active volume of the air. The intensity difference between vacuum and ambient pressure was less than 10% in the case of 50 mm focal length, which was the usual case in our experiment.

4.4 Polymer film evaluations

Table II summarizes results from the polymer films evaluated using our measurement system. For more detail on these films, consult the References listed in Table II.

Polymer films doped with nonlinear optical monomeric materials MNA, DANS, and DMSM are examined. The efficiencies of these monomers were evaluated in section 3 by powder THG and solution THG measurements. Materials were pre-

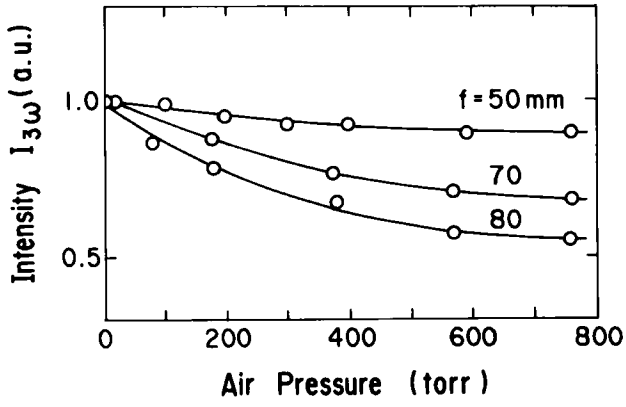

FIGURE 6 THG intensities at λ_p = 1.90 μm for standard silica glass measured in a vacuum chamber, f is focal length of condenser lens.

TABLE II

Evaluated $\chi^{(3)}$ values for several polymer films.

Materials		$\chi^{(3)}$ (10^{-12} esu)	λ_β (μm)	Reference
(silica glass)	SiO_2	0.028	(1.90)	20
monomer – doped polymer	2 wt % MNA / PMMA	0.061	(1.90)	–
	0.1 wt % DANS / PMMA	0.058	(1.90)	–
	10 wt % DMSM / PVA	0.37	(1.90)	–
monomer – pendant polymer	(azo-benzen)	~3.2	(1.90)	22
π – conjugated polymer	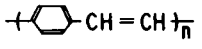	7.8	(1.85)	23
	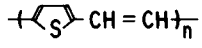	32	(1.85)	24
polydiacetylene	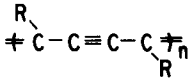			
	solvent – cast film	1.4~5	(1.90)	25
	vac. deposited film	11~380	(1.90)	26-28

pared by dissolving the dopant monomer in methylmethacrylate monomer or vinyl-alcohol monomer, and by polymerizing the solutions. Films were fabricated by casting. The $\chi^{(3)}$ values of MNA/PMMA and DANS/PMMA were small, resulting from the small third-order hyperpolarizability of MNA molecules, and the low concentration of DANS molecules. A relatively large $\chi^{(3)}$ value was obtained in the 10% (*m/m*) DMSM/PVA sample. A higher concentration of non-linear optical monomeric material is achieved by substituting azo-dye molecules as side groups of PMMA or PMA. Monomer concentrations of up to 45% (mol/mol) and $\chi^{(3)}$ value of the order of 10^{-12} esu were realized by this method.

Amorphous π-conjugated conducting polymers of arylene-vinylenes, such as poly (*p*-phenylenevinylene) (PPV) and poly (2,5-thienylenevinylene) (PTV), have potential as large $\chi^{(3)}$ materials. The $\chi^{(3)}$ values were determined to be 7.8×10^{-12} esu and 3.2×10^{-11} esu for cast films of PPV and PTV, respectively. These amorphous polymers have the advantages of easy film fabrication and large film thickness.

Cast films are also available for some polydiacetylenes; however, their measured $\chi^{(3)}$ values are relatively small, as shown in Table II. The largest $\chi^{(3)}$ values were

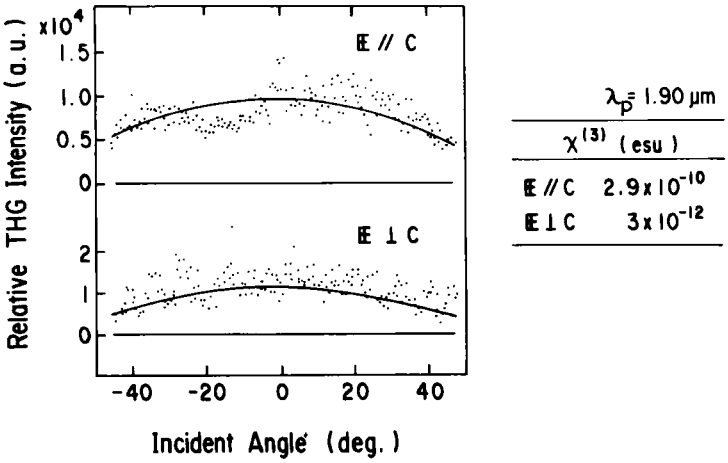

FIGURE 7 THG patterns of the polydiacetylene film, for parallel and perpendicular polarizations to the polymer chain axis.

observed in vacuum-deposited polydiacetylene films. Monomer films were prepared by vacuum deposition onto glass substrates, and the films were then polymerized by UV-light irradiation. $\chi^{(3)}$ values of vacuum-deposited films ranged widely from 1.1×10^{-11} esu to 3.8×10^{-10} esu, depending on the kinds of polydiacetylene materials, presumably corresponding to film qualities such as π-electron conjugation length and spatial order of polymer chains. The largest $\chi^{(3)}$ value was detected in highly oriented polydiacetylene film having urethane-based alkyl chains of $R = (CH_2)_4OCONH(CH_2)_3CH_3$ as side groups.

Figure 7 shows THG patterns of the above polydiacetylene film, for pump-beam polarizations parallel and perpendicular to the polymer chain axis. Fairly large anisotropy of four orders of magnitude was detected in THG intensities, meaning two orders of magnitude anisotropy in $\chi^{(3)}$ values. THG measurement was a very good technique in this case to analyze molecular orientation in the crystal.

5. CONCLUSIONS

Methods to evaluate third-order nonlinear optical susceptibilities by THG measurement have been demonstrated for powder, solution, and film samples. Accurate $\chi^{(3)}$ determination was achieved for film samples by comparing THG intensities with the standard sample, using very simple equations. Several kinds of polymer films were evaluated by this method to be $\chi^{(3)} \approx 10^{-10}$ esu for vacuum deposited polydiacetylene film, 10^{-11} and 10^{-12} esu for arylene-vinylene conducting polymers and monomer-doped polymers, respectively.

Acknowledgments

The authors are grateful to Drs. T. Ikegami, H. Kanbe and H. Hiratsuka for encouragement and discussions. The authors also acknowledge T. Kaino, S. Tomaru, S. Matsumoto, and T. Kurihara of

NTT Opto-electronics Lab., Professors T. Koda, K. Ishikawa, and K. Takeda of the University of Tokyo, and Professors S. Saito and S. Tokito of the University of Kyushu, for supplying organic materials.

References

1. D. J. Williams, "Nonlinear Optical Properties of Organic and Polymeric Materials," ACS Symposium Series 233, American Chemical Society, Washington, D.C., 1983.
2. D. S. Chemla and J. Zyss, "Nonlinear Optical Properties of Organic Molecules and Crystals," Academic Press, Orlando, Florida, 1987.
3. S. D. Smith, *Appl. Opt.*, **25**, 1550 (1986).
4. P. W. Smith, *IEEE Circuits and Devices Magazine*, May, 9 (1987).
5. T. Hattori and T. Kobayashi, *Chem. Phys. Lett.*, **133**, 230 (1987).
6. P. N. Prasad, in "Nonlinear Optical and Electroactive Polymers," (eds. P. N. Prasad and D. R. Ulrich), Plenum Press, New York, 1988, p. 41.
7. F. Kajzar and J. Messier, p. 51 in Reference 2.
8. K. Kubodera and T. Kaino, in "Nonlinear Optics of Organics and Semiconductors," (ed. T. Kobayashi), Springer-Verlag, Berlin, 1989, p. 163.
9. W. Blau, *Opt. Commun.*, **64**, 85 (1987).
10. G. M. Carter, Y. J. Chen and S. K. Tripathy, *Appl. Phys. Lett.*, **43**, 891 (1983).
11. K. Sasaki, K. Fujii, T. Tomioka and T. Kinoshita, *J. Opt. Soc. Am.*, **B5**, 457 (1988).
12. H. Uchiki and T. Kobayashi, in Conference on Lasers and Electro-Optics, Anaheim, WW3 (1988).
13. K. Kubodera, S. Tomaru, H. Kobayashi, T. Kanetake, K. Ishikawa, T. Koda, K. Takeda, Y. Tokura and S. Koshihara, in Topical Meeting on Nonlinear Optical Properties of Materials, Troy, New York, WB1 (1988).
14. J. L. Oudar, *J. Chem. Phys.*, **67**, 446 (1977).
15. T. Kobayashi, H. Ohtani and K. Kurokawa, *Chem. Phys. Lett.*, **121**, 356 (1985), T. Kobayashi, M. Terauchi and H. Uchiki, *Chem. Phys. Lett.*, **126**, 143 (1986), and H. Uchiki and T. Kobayashi, *Chem. Phys. Lett.*, **128**, 559 (1986).
16. B. F. Levine and C. G. Bethea, *J. Chem. Phys.*, **65**, 2429 (1976).
17. C. Sauteret, J. P. Hermann, R. Frey, F. Pradere, J. Ducuing, R. H. Baughman and R. R. Chance, *Phys. Rev. Lett.*, **36**, 956 (1976).
18. B. F. Levine, C. G. Bethea, C. D. Thurmond, R. T. Lynch and J. L. Bernstein, *J. Appl. Phys.*, **50**, 2523 (1979).
19. G. R. Meredith, p. 27 in Reference 1.
20. G. R. Meredith, B. Buchalter and C. Hanzlik, *J. Chem. Phys.*, **78**, 1533 (1983).
21. J. F. Ward and G. H. C. New, *Phys. Rev.*, **185**, 57 (1969).
22. S. Matsumoto, K. Kubodera, T. Kurihara and T. Kaino, *Appl. Phys. Lett.*, **51**, 1 (1987).
23. T. Kaino, K. Kubodera, S. Tomaru, T. Kurihara, S. Saito, T. Tsutsui and S. Tokito, *Electron. Lett.*, **23**, 1095 (1987).
24. T. Kaino, K. Kubodera, H. Kobayashi, T. Kurihara, S. Saito, T. Tsutsui, S. Tokito and H. Murata, *Appl. Phys. Lett.*, **53**, 2002 (1988).
25. T. Kurihara, K. Kubodera, S. Matsumoto and T. Kaino, *Polymer Preprints, The Society of Polymer Science, Japan*, **36**, 1157 (1987), *in Japanese.*
26. S. Tomaru, K. Kubodera, S. Zembutsu, K. Takeda and M. Hasegawa, *Electron. Lett.*, **23**, 595 (1987).
27. S. Tomaru, K. Kubodera, T. Kurihara and S. Zembutsu, *Jpn. J. Appl. Phys.*, **26**, L1657 (1987).
28. T. Kanetake, K. Ishikawa, T. Hasegawa, T. Koda, K. Takeda, M. Hasegawa, K. Kubodera and H. Kobayashi, *Appl. Phys. Lett.*, **54**, 2287 (1989).